

Emission line activity in type 2 quasars from the Sloan Digital Sky Survey

M. Villar-Martín¹, A. Humphrey^{2,3}, A. Martínez-Sansigre⁴, M. Pérez-Torres¹
L. Binette^{3,5}, X.G. Zhang^{3,6}

¹*Instituto de Astrofísica de Andalucía (CSIC), Aptdo. 3004, Granada, Spain*

²*Korea Astronomy and Space Science Institute, 61-1, Hwaam-dong, Yuseong-gu, Daejeon, Republic of Korea 305-348*

³*Instituto de Astronomía, Universidad Nacional Autónoma de México, Ap. 70-264, 04510, DF, México*

⁴*Max-Planck-Institut für Astronomie, Königstuhl 17, D-69117 Heidelberg, Germany*

⁵*Département de Physique, de Génie Physique et d'Optique, Université Laval, Québec, QC, G1K 7P4, Canada*

⁶*Max-Planck-Institut für Astrophysik, Karl Schwarzschild-Str. 1, 85748 Garching, Germany*

Accepted 2008 July 29. Received 2008 July 29; in original form 2008 February 1

ABSTRACT

We have compared the optical emission line ratios of type 2 quasars from Zakamska et al. with standard AGN photoionization model predictions, Seyfert 2s, HII galaxies, and narrow line FRII radio galaxies. Moderate to high ionization narrow line radio galaxies and Seyfert 2s are indistinguishable from type 2 quasars based on their optical line ratios. The standard AGN photoionization models, widely discussed for other type 2 AGNs, can reproduce successfully the loci and trends of type 2 quasars in some of the main diagnostic diagrams. These models are not exempt of problems and the discrepancies with the data are the same encountered for other type 2 AGNs. As for these, realistic models must take into account a range of cloud properties, as widely demonstrated in the literature.

The Zakamska et al. sample is strongly biased towards objects with high line luminosities ($L[\text{OIII}] > 10^{42} \text{ erg s}^{-1}$). We have found that stellar photoionization is obvious in a fraction of objects (3 out of 50) which are characterized by low $[\text{OIII}]$ luminosities compared with most type 2 quasars in the sample. We suggest that if the sample were expanded towards lower line luminosities ($\sim 10^{40-42} \text{ erg s}^{-1}$) stellar photoionization might be evident much more frequently.

We explore an alternative scenario to pure AGN photoionization in which a varying contribution of stellar ionized gas contributes to the line fluxes. Although the models presented here are rather simplistic and not strong quantitative results can be extracted regarding the relative contribution of stellar vs. AGN photoionization, our results suggest that adding a varying contribution of stellar photoionized gas works in the right direction to solve most of the problems affecting the standard AGN photoionization models. The “temperature problem”, on the other hand remains.

Key words: galaxies: active; quasars: general; quasars: emission lines

1 INTRODUCTION

Type 2 active galactic nuclei (AGNs) are those AGNs whose permitted and forbidden lines have similar values of full width at half maximum (FWHM). In many cases (e.g. Seyfert 2 galaxies) this can be explained as a consequence of obscuration of the central region by large column densities of gas and dust. In the standard unification model the obscuring structure is toroidal in shape so that the view to the inner nuclear region is blocked for some orientations (Antonucci 1993). According to this model, certain classes of type 1 and type 2 AGNs are the same entities, but have different orientations relative to the observer line of sight. If this model

is valid for the most luminous AGNs (quasars), there must exist a high-luminosity family of type 2 quasars.

The existence of such an object class was predicted a long time ago, but it has been only in the last few years that type 2 quasars have been discovered in large quantities in X-ray, mid-IR (Martínez-Sansigre et al. 2005, Szokoly et al. 2004) and optical surveys (Zakamska et al. 2003). Zakamska et al. (2003) identified ~ 145 objects in the redshift range $0.3 \lesssim z \lesssim 0.8$ in the Sloan Digital Sky Survey (SDSS; York et al. 2000) with the high ionization narrow emission line spectra characteristic of type 2 AGNs and narrow line luminosities typical of type 1 quasars (see also Reyes et al. 2008). Their IR and X-ray properties are consistent with their interpretation as powerful obscured AGN (Ptak et al. 2006, Zakamska

et al. 2004). They show a wide range of X-ray luminosities and obscuring column densities. About 40 objects in their sample were detected with IRAS and have infrared luminosities among the most luminous quasars at similar redshift. The host galaxies are ellipticals, although with irregular morphologies, and the nuclear optical emission is highly polarized (Zakamska et al. 2006). The detection rate in radio ($\sim 10\%$, Zakamska et al. 2004; Vir Lal & Ho 2007) is consistent with that of other AGN types.

Spectroscopic studies of type 2 quasars have focused so far on identifying emission lines, measuring some basic parameters (line luminosities, redshift, line widths) and searching for correlations among them and with other observables (equivalent widths, color magnitudes, radio luminosities, etc). All this is critical to classify the objects, to investigate the nature of the powering mechanism, the obscuring structure and, ultimately, test the validity of the unification models (e.g. Reyes et al. 2008).

However, little work has been done to characterize the gaseous and ionization properties of type 2 quasars. Given this lack of knowledge, the primary goal of the work presented here is to use the emission line information to study the excitation mechanism, the physical conditions and ionization properties of the gas.

Detailed spectroscopic studies of other active galaxy types, such as narrow line radio galaxies (NLRGs, e.g. Robinson et al. 1987) have allowed during the last few decades the characterization of the chemical abundances of the gas, the ionization mechanism, the physical and kinematic properties, etc. Similar work must be done for type 2 quasars. These studies will ultimately provide valuable information about the formation process of the host galaxy, the star forming and chemical enrichment histories and the origin of the nuclear activity (e.g. Tadhunter, Fosbury & Quinn 1989, Villar-Martín et al. 2005, Humphrey et al. 2008). An important disadvantage of NLRG over type 2 quasar studies is that the radio activity, via jet-gas interactions, imprints important distortions on the properties of the ionized gas making it difficult to investigate the intrinsic properties of the host galaxy and environment, as well as the chemical abundances and the nature of the excitation mechanism (e.g. Tadhunter 2002). The study of radio-quiet type 2 quasars should not suffer from such effects.

Throughout this paper we assume $\Omega_\Lambda = 0.73$, $\Omega_m = 0.27$ and $H_0 = 71 \text{ km s}^{-1} \text{ Mpc}^{-1}$.

2 THE OBJECT SAMPLE

The objects studied in this paper are a sub-sample of candidate type 2 quasars from the Sloan Digital Sky Survey (SDSS) selected by Zakamska et al. (2003) in the redshift range $0.3 \lesssim z \lesssim 0.8$ (~ 145 objects). The selection criteria applied by Zakamska et al. (2003) are listed below (notice that not necessarily all criteria apply to all objects. See Zakamska et al. 2003 for more detailed information)).¹

- $i \leq 19.1$
- $0.3 < z < 0.83$
- Signal to noise ratio > 7.5
- Equivalent width (EW) of $[\text{OIII}] \geq 4 \text{ \AA}$
- Luminosity of $[\text{OIII}]$, $L([\text{OIII}]) \geq 3 \times 10^8 L_\odot$
- Full width at half maximum, $\text{FWHM}(\text{H}\beta) < 2000 \text{ km s}^{-1}$

- Selection of active galaxies among emission line galaxies, based on line ratio criteria (different line ratios depending on z)
- Other signs of AGN activity such as the detection of the high ionization lines $[\text{NeV}] \lambda\lambda 346, 3426$ and/or $\text{FWHM}([\text{OIII}]) > 400 \text{ km s}^{-1}$.

The sub-sample studied here contains 50 type 2 quasars, which have been selected to span the full z range and the full $[\text{OIII}]$ luminosity range ($\geq 3 \times 10^8 L_\odot$) of the original type 2 quasar sample. We did not set constraints on the line equivalent widths, although the selection criteria on the original sample do contain an EW criterion, as stated above.

The spectra were corrected for Galactic extinction. A galaxy template spectrum was subtracted for objects with low line EWs, to correct for possible underlying stellar and interstellar absorption (Zhang, Dultzin-Hacyan & Wang 2007). This procedure was necessary for a small fraction of objects ($\sim 15\%$ only).

The spectra were not corrected for internal dust reddening because such correction was not possible for all objects. It should not affect our conclusions since we will compare our results with previous works on other AGN types (Seyfert 2s, radio galaxies), in which no internal extinction correction was applied either.

3 ANALYSIS AND RESULTS

We investigate in this section the dominant ionizing mechanism of the optical line emitting gas in the type 2 quasar sub-sample: AGN vs. stellar photoionization.

We will ignore shocks in our discussion as an alternative ionization mechanism (e.g. Dopita & Sutherland 1996). In our sub-sample, 44 out of the 47 objects for which radio information is available are radio quiet (i.e. $L_{1.4\text{GHz}} < 10^{31} \text{ erg s}^{-1} \text{ Hz}^{-1} \text{ sr}^{-1}$) and therefore, shocks induced by the radio structures are not expected to play a significant role in the ionization of the gas (e.g. Clark et al. 1998, Villar-Martín et al. 1999). In the vast majority of the type 2 quasars in the sample considered here, the bulk of the line profiles is characterized by rather quiescent kinematics, rather than perturbed, as one would expect if shocks were present.

3.1 AGN photoionization

We show in Fig. 1 several diagnostic diagrams involving optical emission lines in which we plot the location of the SDSS type 2 quasar sub-sample (green, solid circles and blue solid triangles). For comparison, we plot in the same diagrams the locus of HII galaxies from the catalogue of Terlevich et al. (1991) (magenta small symbols). These are absent in diagrams involving the HeII and $[\text{NeV}]$ because such lines are rarely detected in this object class.

The solid lines represent the standard 2U sequence of photoionization models, built with the multipurpose code MAPPINGS Ic (Binette, Dopita & Tuohy 1985; Ferruit et al. 1997) that reproduces some of the main properties of the emission line spectra of narrow line radio galaxies at different redshifts (e.g. Robinson et al. 1987, Humphrey et al. 2008). The ionizing continuum is a power law of index $\alpha=1.5$ ($F_\nu \propto \nu^{-\alpha}$), with a cut off energy of

² $U = \frac{Q}{4 \pi r^2 n_H c}$, where Q is the ionizing photon luminosity of the source, r is the distance between the cloud and the ionizing source, n_H is the hydrogen density at the illuminated face of the cloud and c is the speed of light.

¹ Throughout the paper the emission lines will be named as follows: $[\text{OIII}]$ for $[\text{OIII}]\lambda 5007$; $[\text{OII}]$ for $[\text{OII}]\lambda 3727$; $[\text{NII}]$ for $[\text{NII}]\lambda 6583$; $[\text{NeV}]$ for $[\text{NeV}]\lambda 3426$; $[\text{NeIII}]$ for $[\text{NeIII}]\lambda 3689$; HeII for $\text{HeII}\lambda 4686$.

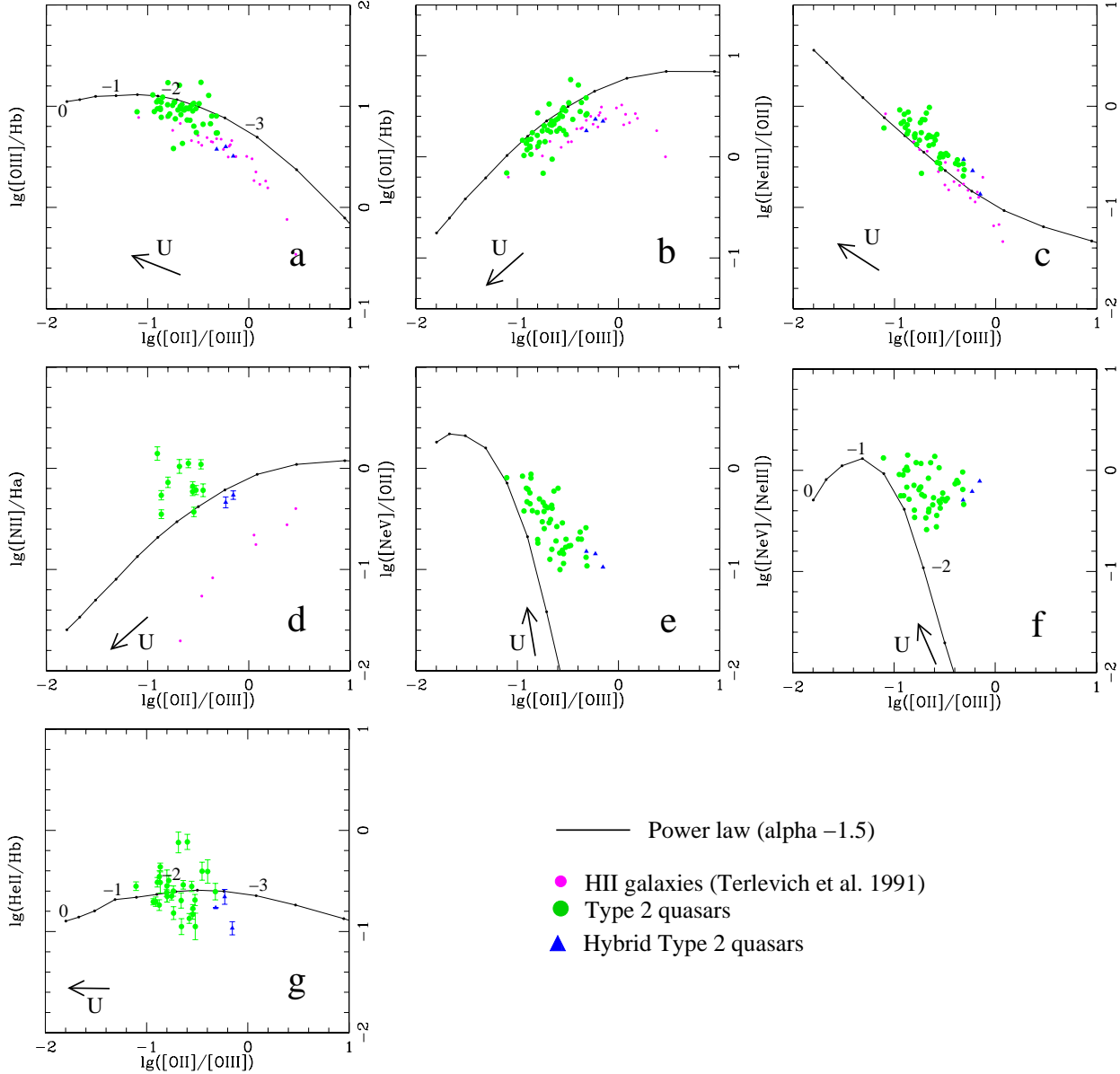


Figure 1. Loci of type 2 quasars in diagnostic diagrams involving the main optical emission lines detected in most spectra. Hybrid objects are those with signatures of stellar photoionization. The solid line is the standard sequence of solar metallicity AGN photoionization models along which the ionization parameter U varies. $\lg(U)$ values are shown for some models in several diagrams. The arrows indicate the sense of increasing U . Error bars are shown in those diagrams where the measurement errors could have an impact on our interpretation and conclusions (*d* and *g*). In all other diagrams the errorbars are in general smaller. The comparison with the models and HII galaxies suggests that in general, AGN photoionization plays an important role in ionizing the gas and the ionization parameter varies from object to object. On the other hand, the standard AGN sequence shows some discrepancies with the data (e.g. diagrams *d*, *e*, *f*, *g*) which are the same encountered for other type 2 AGNs. Stellar photoionization is apparent in a small fraction of objects (hybrid object).

50 keV. The clouds are considered to be isobaric, plane-parallel, dust-free ionization-bounded slabs of density $n = 100 \text{ cm}^{-3}$ at the illuminated face and characterized by solar abundances (Anders & Grevesse 1989). Since the SDSS spectra integrate the emission from nuclear (i.e., the narrow line region, NLR) and (possibly) extended gas, a range of cloud densities is expected with values as high as 10^6 cm^{-3} or more. Given the low critical density of $[\text{OII}]\lambda 3727$ ($\sim 3000 \text{ cm}^{-3}$), such high densities will pose difficulties to reproduce the observed strength of $[\text{OII}]$ relative to other emission lines, which suggest a substantial contribution to the in-

tegrated spectrum of a low density component. Thus, although it is clear that assuming a single density is a rough simplification (characteristic on the other hand of the standard AGN sequence discussed in numerous papers), we will assume $n_e = 100 \text{ cm}^{-3}$ as a representative density of the gas within the SDSS aperture and mention the possible impact of higher densities when necessary.

There are several diagrams which are specially sensitive to the ionization parameter U , in the sense that for a specific ionization mechanism, the line ratios involved are strongly influenced by a change in U . These diagrams are *a*, *b*, *c*, *e* and *f* (Fig. 1). The mod-

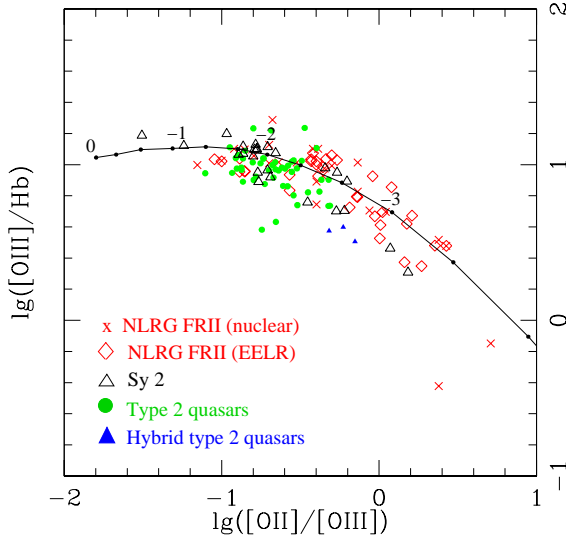


Figure 2. Comparison among type 2 quasars, Seyfert 2s and narrow line FR II radio galaxies (nuclear and extended emission line regions, EELR). The solid line is the AGN model sequence, as in Fig. 1. The three object classes overlap in the area of the diagram with $\lg(U) \gtrsim -2.6$. The lack of type 2 quasars with $\lg([OIII]/H\beta) \lesssim 0.5$ is due to the selection criteria.

els shows the large shift along the sequence expected as U varies. Looking at the distribution of data points in diagrams *a*, *b*, *c* and *e*, type 2 quasars follow a sequence whose shape can be accounted for by a variation in U . Most objects have $\lg(U)$ values in the range $[-2.7, -1.7]$

There are several arguments that suggest that AGN photoionization plays an important role in ionizing the gas:

- The shape and location of the sequence defined by type 2 quasars is adequately accounted for by the AGN models in the *a*, *b* and *c* diagrams.
- Type 2 quasars have similar line ratios than Seyfert 2 and narrow line radio galaxies. We compare in Fig. 2 the loci of type 2 quasars, Seyfert 2 (black open triangles) and radio galaxies (red diamonds for the extended emission line regions (EELR) and red 'x' for the nuclear regions) in the $[OIII]/H\beta$ vs. $[OII]/[OIII]$ diagnostic diagram. This diagram is chosen because of its high sensitivity to the ionization level of the gas, whose variation, as proposed above, can explain the trends defined by type 2 quasars in those diagnostic diagrams with the highest sensitivity to U . The data for most Seyfert 2s were collected from Koski (1978). Some more line ratios were taken from papers on individual sources (e.g. Bennert et al. 2006, Ferruit et al. 1999, Contini et al. 2002, Allen et al. 1999, Diaz et al. 1988, Kraemer & Crenshaw 2000). The radio galaxy data set is the same as in Holt (2006). None of these line ratios have been corrected for internal reddening. Fig. 2 shows that type 2 quasars overlap in the diagram with radio galaxies with moderate and high ionization level ($\lg(U) \gtrsim -2.6$) and with most Seyfert 2 galaxies. This suggests similar ionization mechanism, ionizing continuum shape, physical properties of the gas and a similar range of chemical abundances. The lack of type 2 quasars with $\lg([OIII]/H\beta) \lesssim 0.5$ is due to the selection criteria (see Zakamska et al. 2003).

- Type 2 quasars are in general clearly separated from HII galaxies (see diagrams *a*, *b* and *d*). This is particularly evident in diagram *d*, involving the $[NII]/H\alpha$ ratio (see also Fig. 3). This is also evident in Fig. 3, which shows one of the most efficient diagrams at separating active galaxies and HII galaxies (Baldwin, Philips &

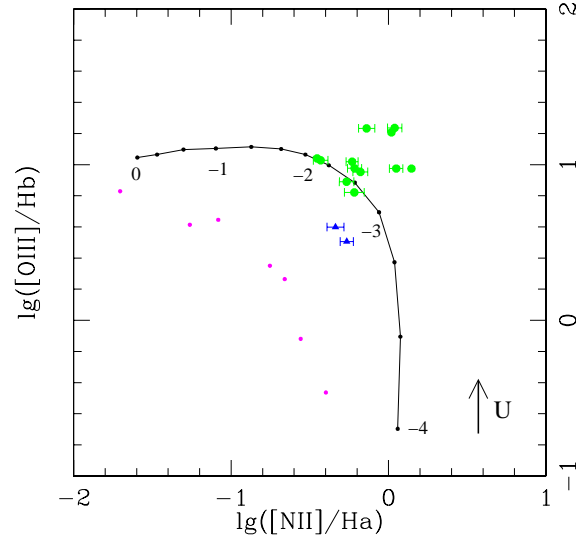


Figure 3. Type 2 quasars and HII galaxies plotted in Baldwin, Philips & Terlevich (1982) diagnostic diagram to classify emission line extragalactic objects. Type 2 quasars are clearly separated from HII galaxies. They occupy the area of the diagrams where typical type 2 AGNs lie. Symbols and lines as in Fig. 1.

Terlevich 1982). The $[NII]/H\alpha$ ratio was measurable only for 30% of the objects. In a few cases, the lines are in a very noisy part of the spectrum due to strong sky residuals. For most spectra, they are outside the observed spectral range. In spite of this, the separation from HII galaxies (also with scarce $[NII]/H\alpha$ measurements) is evident and type 2 quasars occupy the area of the diagram where active galaxies lie (see Fig. 5 in Baldwin, Philips & Terlevich 1982). The harder continuum in active galaxies, produces a much deeper partially ionized region in which low ionization lines, such as $[NII]$ are efficiently excited. Although less evident, a similar effect accounts for the fact that the sequence defined by HII galaxies in diagrams *a* and *b* is shifted down relative to that defined by the type 2 quasars.

- $[NeV]$ and/or $HeII$ are detected in all objects, while these lines are rarely found in the spectra of star forming galaxies.
- The line luminosities of type 2 quasars are characteristic of quasars rather than of star forming objects (Zakamska et al. 2003).

In spite of the general success of the standard AGN photoionization models to explain the emission line spectra of type 2 quasars, the models encounter some problems, which are exactly those found in studies of other type 2 AGNs (e.g. Groves, Dopita & Sutherland 2004; Binette, Wilson & Storchi-Bergmann 1996; Robinson et al. 1987).

A. High ionization lines imply higher U values than low ionization lines

The diagrams in Fig. 1 show that low and high ionization lines require different values of U . This is specially clear in diagrams *e* and *f* involving the $[NeV]$ line, where type 2 quasars are shifted relative to the AGN model sequence. While the $[NeV]$ ratios imply $\lg(U)$ in the range $[-1.8, -1]$, the implied range of values in diagrams *a*, *b* and *c* is $[-2.7, -1.6]$. As for other AGN types at different redshifts (e.g. Humphrey et al. 2008, Binette, Wilson & Storchi-Bergmann 1996), the models that reproduce some of the main line ratios under-predict the highest ionization lines ($[NeV]\lambda 3426$ in our case).

Since the faint $[NeV]$ line is detected in most objects plotted in Fig. 1, the discrepancy is not the result of different diagrams

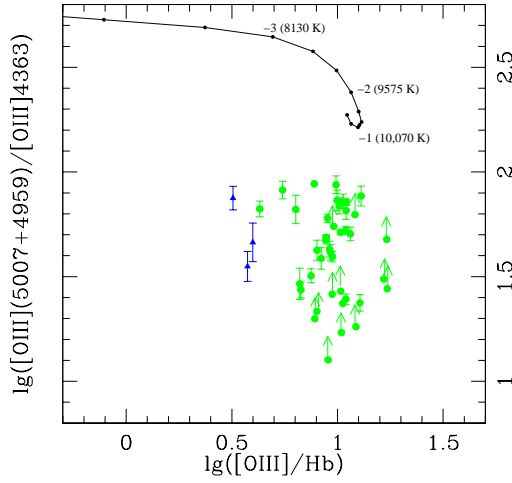


Figure 4. The $[\text{OIII}]\lambda\lambda 5007,4959/[\text{OIII}]\lambda 4363$ temperature sensitive ratio predicted by the AGN photoionization models is well above the measured values. Errors cannot account for such large discrepancy. Arrows indicate lower limits. Symbols and lines as in Fig. 1.

showing different sub-samples. The problem is found in individual objects.

This cannot be accounted for by reddening effects. Correcting for reddening would produce higher $[\text{NeV}]/[\text{OII}]$ and $[\text{NeV}]/[\text{NeIII}]$ that would result on larger U values. On the other hand, $[\text{OII}]/[\text{OIII}]$ would also become larger, implying lower U values. Therefore, the discrepancy would be worse.

B. Too low electronic temperatures

We have plotted in Fig. 4 the temperature sensitive $[\text{OIII}]\lambda\lambda 5007,4959/[\text{OIII}]\lambda 4363$ ratio vs. $[\text{OIII}]/\text{H}\beta$. The arrows correspond to objects for which $[\text{OIII}]\lambda 4363$ was not detected and only upper limits could be estimated. For all objects the predicted and measured values of $[\text{OIII}]\lambda\lambda 5007,4959/[\text{OIII}]\lambda 4363$ are discrepant by at least a factor of 2 (a shift of >0.3 in \lg). This cannot be accounted for by measurement errors (see Fig. 4) or reddening effects, since correcting for this would result on even lower $[\text{OIII}]\lambda\lambda 5007,4959/[\text{OIII}]\lambda 4363$ ratios.

Higher densities can explain low $[\text{OIII}]\lambda\lambda 5007,4959/[\text{OIII}]\lambda 4363$ values consistent with the data, but produce strong discrepancies with other line ratios. As an example, models with $n=10^5 \text{ cm}^{-3}$ produce $\lg([\text{OIII}]\lambda\lambda 5007,4959/[\text{OIII}]\lambda 4363) \leq 2$, as measured for many type 2 quasars. However, for such models $[\text{OII}]/[\text{OIII}] \leq 0.02$, $[\text{OII}]/\text{H}\beta \leq 0.3$ (much lower than the measured values, Fig. 1) and $[\text{OIII}]/\text{H}\beta \geq 18$ (higher than measured, Fig. 1). High densities *only*, therefore, in general do not solve the problem.

In the low density limit (Osterbrock 1989), this discrepancy implies that the models predict too low electron temperatures: $T_e \leq 11000 \text{ K}$ for all models of the U sequence, while the measured line ratios imply $T_e \gtrsim 15000 \text{ K}$, being >20000 in several cases, errors considered. The same problem has been discussed in detail for other type 2 AGNs (e.g. Binette, Wilson & Storchi-Bergmann 1996, Robinson et al. 1987).

C. Too small scatter of the $\text{HeII}/\text{H}\beta$ ratio

The data present a large $\text{HeII}/\text{H}\beta$ scatter inconsistent with the standard AGN sequence (Fig. 1 bottom panel), which is not due to errors in the measurements, neither reddening effects. There are

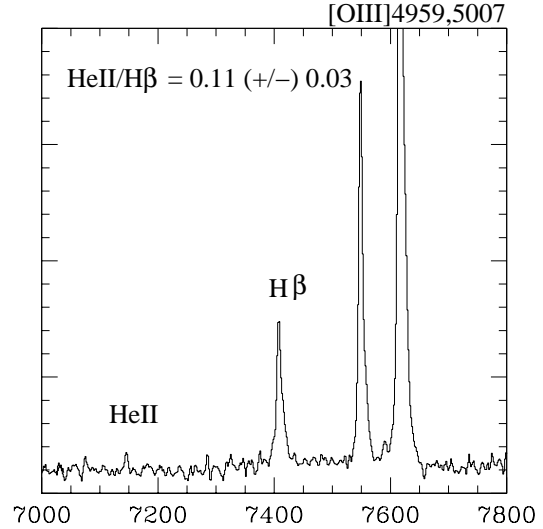
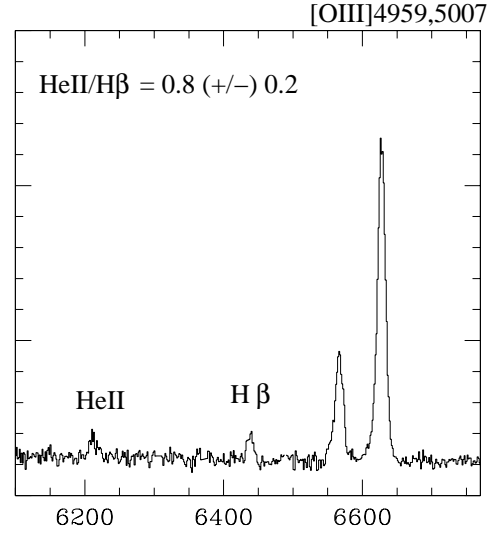


Figure 5. Examples of objects with very high (top) and very low (bottom) $\text{HeII}/\text{H}\beta$ ratios.

objects with too high and objects with too low $\text{HeII}/\text{H}\beta$ ratios compared with the model predictions (see Fig. 5). Such large scatter has been observed also in low z radio galaxies (e.g. Robinson et al. 1987).

D. Too strong $[\text{NII}]$ emission

The $[\text{NII}]/\text{H}\alpha$ vs. $[\text{OII}]/[\text{OIII}]$ diagram (Fig. 1) shows a very large scatter in the $[\text{NII}]/\text{H}\alpha$ ratio inconsistent with the standard AGN (solar metallicity) predictions which again cannot be explained by errors in the measurements or reddening effects. For a large fraction of objects, the $[\text{NII}]$ emission is too strong. Given that this ratio is a direct metallicity indicator, rather than being a problem for photoionization models, the large range of values suggests that the nitrogen/hydrogen ratio varies substantially within the sample. Nitrogen is likely to be overabundant in those objects with large $[\text{NII}]/\text{H}\alpha$ values (e.g. Robinson et al. 1987).

3.2 Alternative AGN scenarios.

Possible solutions to these problems have been extensively discussed in the literature for more than 20 years. We present here

a brief summary of the main alternative AGN photoionization scenarios.

- Mixture of matter and radiation bounded clouds (e.g. Binette, Wilson & Storchi-Bergmann 1996; Viegas & Prieto 1992). Contrary to ionization bounded (IB) clouds, matter bounded (MB) clouds are not sufficiently thick to absorb all the ionizing radiation. In the scenario proposed by Binette, Wilson & Storchi-Bergmann (1996) the IB component sees a spectrum modified by absorption within the MB component.

- Locally optimally emitting clouds. The failure of “simple” AGN photoionization models to describe the narrow emission line spectrum of Seyfert 2 galaxies lead Baldwin et al. (1995) and Ferguson et al. (1997) to propose an alternative scenario in which the integrated narrow-line spectrum can be predicted by an integration of an ensemble of clouds with a wide range of gas densities and distances from the ionizing source with an appropriate covering factor and distribution. For each line, only a narrow range of density and distance from the continuum source results in maximum reprocessing efficiency, corresponding to “locally optimally emitting clouds”.

- Dusty, radiation-pressure dominated photoionization models (Groves, Dopita & Sutherland 2004, Dopita et al. 2002). In these models, dust and the radiation pressure acting upon it provide the controlling factor in moderating the density, excitation and surface brightness of the photoionized gas. Additionally, photoelectric heating by the dust modifies the gaseous temperature structure.

- Humphrey et al. (2008) discuss in detail the need for a mixture of cloud properties (a range in U) in individual objects to explain the UV and optical rest-frame line ratios of high z radio galaxies.

3.3 Stellar photoionization

There are 3 objects, highlighted as blue triangles in Fig. 1, which show hybrid properties of both AGNs and HII galaxies. Their line ratios in diagrams *a*, *b* and *c* fit better a classification as HII galaxies. Their lines are also relatively narrow compared with most objects in the sample, for which the median value is 530 km s^{-1} while the hybrid objects have $\text{FWHM}[\text{OIII}] < 470 \text{ km s}^{-1}$. They show among the lowest $[\text{OII}]/[\text{OIII}]$ and $[\text{OIII}]/\text{H}\beta$ values in the sample.

On the other hand, they show some features characteristic of active galaxies: they emit $[\text{NeV}]$ and HeII (Fig. 1) and have large line luminosities ($L[\text{OIII}] \gtrsim 10^{42} \text{ erg s}^{-1}$). The two objects for which $[\text{NII}]$ was measured occupy an intermediate region in the $[\text{OIII}]/\text{H}\beta$ vs. $[\text{NII}]/\text{H}\alpha$ diagram (Fig. 3) between HII galaxies and AGNs. We will call these hybrid objects.

Based on the arguments exposed in the previous sections, AGN photoionization must play an important role in the ionization of the gas in type 2 quasars in this sample. The discrepancies of the standard AGN sequence show that a range of ionization and probably physical properties must exist within the type 2 quasar sample. An internal range of cloud properties (e.g. density range, matter and bounded clouds, ionization level etc) is also likely to exist in individual objects. This is only natural, one cannot expect identical gas and continuum properties in all quasars, or ensembles of identical clouds in individual objects. As we discussed above, more sophisticated models that take this into account solve the problems of the standard AGN sequence.

However, the emission line spectra of the three hybrid objects suggests that stellar photoionization might also be present with different degrees of importance relative to AGN photoionization from object to object. Interestingly, although uncommonly high $[\text{OIII}]$

luminosities for HII galaxies, the hybrid objects are at the lowest end of $L[\text{OIII}]$ values within the type 2 quasar sample ($\lesssim 2 \times 10^{42} \text{ erg s}^{-1}$, while the median value is $\sim 6 \times 10^{42} \text{ erg s}^{-1}$). This tentatively suggests that low line luminosities might be associated with relatively stronger stellar photoionization.

We investigate next whether a contribution of stellar photoionized gas could solve the problems of the standard AGN models discussed above. For simplicity, we have assumed that the total flux of a given line is due to the added contribution of the flux emitted by an AGN photoionized component (represented by the standard AGN sequence) plus the flux emitted by a stellar photoionized component. To represent the spectrum emitted by this gas, we have used the real spectra of a variety of HII galaxies in Terlevich et al. (1991) catalogue. We find from this study that the stellar ionized component must have $[\text{OII}]/[\text{OIII}] \gtrsim 1$ in order to shift the models in the right direction in the diagrams.

As an example we take UM448. The reason to choose this particular HII galaxy is that it fulfills the $[\text{OII}]/[\text{OIII}] \gtrsim 1$ requirement and has reported measurements of $[\text{OIII}]/\lambda 4363$. Unfortunately, as for all other objects in the catalogue with $[\text{OII}]/[\text{OIII}] \gtrsim 1$, HeII is not measured.

The flux of any line $Flux^{tot}$ relative to $\text{H}\beta^{tot}$ is given by:

$$\frac{Flux^{tot}}{\text{H}\beta^{tot}} = \frac{Flux^* + Flux^{AGN}}{\text{H}\beta^* + \text{H}\beta^{AGN}}$$

where $Flux^*$ and $\text{H}\beta^*$ are respectively the flux of the line and the flux of $\text{H}\beta$ emitted by the stellar ionized gas. $Flux^{AGN}$ and $\text{H}\beta^{AGN}$ are the flux of the line and that of $\text{H}\beta$ emitted by gas ionized by the AGN.

Let us define $x = \frac{\text{H}\beta^*}{\text{H}\beta^{AGN}}$ and rearrange:

$$\frac{Flux^{tot}}{\text{H}\beta^{tot}} = \frac{\frac{Flux^{AGN}}{\text{H}\beta^{AGN}} + x \frac{Flux^*}{\text{H}\beta^*}}{1 + x}$$

We assume $[\text{NeV}]/\text{H}\beta^* \ll [\text{NeV}]/\text{H}\beta^{AGN}$. When detected, $\text{HeII}/\text{H}\beta^*$ in HII galaxies is often in the range ~ 0.02 - 0.1 (values as high as 0.4 are also possible, but are more typical of objects with very small $[\text{OII}]/[\text{OIII}] \lesssim 0.2$ values). We will assume $\text{HeII}/\text{H}\beta^* = 0.04$. Using a different value within the expected range does not change our conclusions.

We now create hybrid models by adding the stellar emission line spectrum to the AGN standard sequence of models and changing the x value from sequence to sequence (see equation above). The ionization parameter U of the AGN photoionized gas (as in the standard AGN sequence) changes along each sequence. The results are shown in Figs. 6, 7 and 8 as red dashed-lines.

We find that by varying the relative contribution of the stellar to the AGN photoionized gas:

- The discrepancy affecting the high and low ionization lines disappears (Fig. 6, panels *e* and *f*).
- The large scatter observed in the $\text{HeII}/\text{H}\beta$ diagram towards low values is now reproduced (Fig. 6, panel *g*).
- The highest $\text{HeII}/\text{H}\beta$ values (~ 0.8 for two objects) cannot be reproduced by the models (Fig. 6, panel *g*). To solve this problem with the stellar photoionized component, this should show similarly high $\text{HeII}/\text{H}\beta$ ratios, which are extreme even for active galaxies. We notice this is also a problem for Groves, Dopita & Sutherland (2004) models, which require extremely high gas metallicities $\sim 4 Z_{\odot}$. No models in Ferguson et al. (1997) reach these high $\text{HeII}/\text{H}\beta$ values either (see Fig. 3b in their paper). A strong contribution

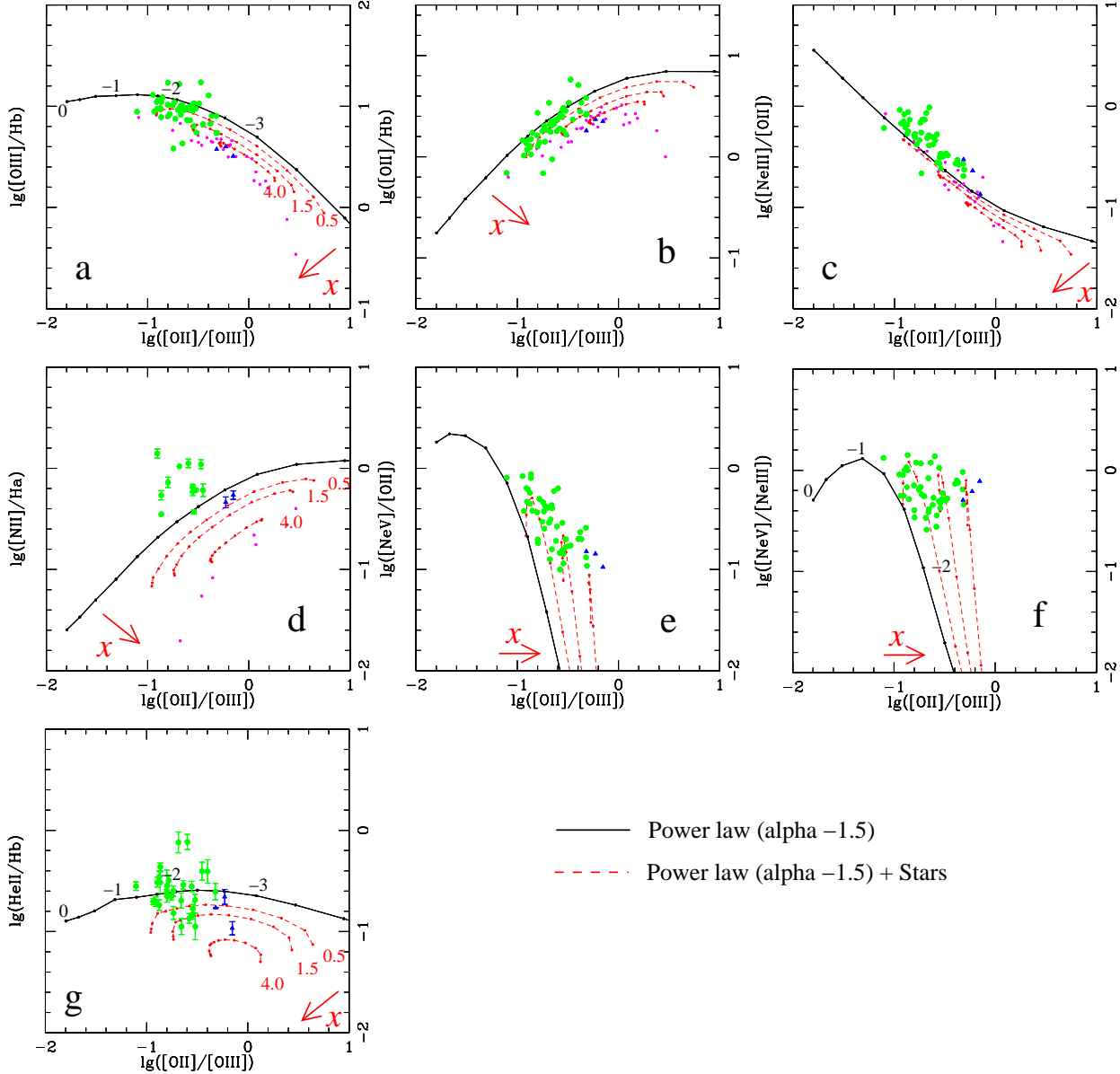


Figure 6. As Fig. 1, adding the hybrid AGN+stellar models (red, dashed lines) for different x values shown in red (0.5, 1.0 and 4.0). The AGN sequence (black solid line) corresponds to $x=0$, i.e., the line fluxes are emitted by gas purely photoionized by the AGN. The arrows indicate the sense of increasing x .

of matter bounded clouds to the integrated spectrum solves the problem (Binette et al. 1996). Given the scarcity of these extreme $\text{HeII}/\text{H}\beta$ ratios in type 2 AGNs in general, we wonder whether these two specific type 2 quasars are particularly rare.

- Although the temperature problem is partially alleviated (Fig. 7), the hybrid models cannot explain the small $[\text{OIII}]\lambda\lambda 5007, 4959/[\text{OIII}]\lambda 4363$ measured in the quasar sample. Given the saturation of this line ratio at high electron temperatures (Osterbrock 1989), not even unrealistically high electron temperatures of a dominant stellar photoionized gas would solve the problem. Notice that Binette et al. (1997) warned about the need for higher densities if the NLR dominates the emission, which would result in lower $[\text{OIII}]\lambda\lambda 5007, 4959/[\text{OIII}]\lambda 4363$ ratios for a given electron temperature.

- The $[\text{NII}]/\text{H}\alpha$ ratio is still too low compared with the obser-

vations. Adding the stellar ionized component only makes things worse (Fig. 6, panel *d* and Fig. 8). However, as explained before, this could be suggestive of an overabundance of nitrogen.

Another test for the stellar photoionization scenario consists of checking whether the measured continuum level is consistent with that expected for the stellar population responsible for $\text{H}\beta^*$. Let us consider the objects with the largest x values. This is the case of the hybrid objects, for which according to the exercise presented here, $x \sim 4$ (see Fig. 6). For these three objects the $\text{H}\beta$ luminosity is in the range $\sim 3\text{--}6 \times 10^{41} \text{ erg s}^{-1}$. We will assume $L(\text{H}\beta) = 4.5 \times 10^{41} \text{ erg s}^{-1}$. If 80% is due to stellar photoionized gas then $L(\text{H}\beta^*) = 3.6 \times 10^{41} \text{ erg s}^{-1}$, rather similar to that of UMM448, $L(\text{H}\beta) = 7.9 \times 10^{40} \text{ erg s}^{-1}$. The rest frame $\text{H}\beta$ EW in the hybrid type 2 quasars is in the range $\sim 32\text{--}38 \text{ \AA}$, implying EW values for $\text{H}\beta^* \sim 25\text{--}30 \text{ \AA}$, quite similar to that measured in UMM448 (43 \AA ,

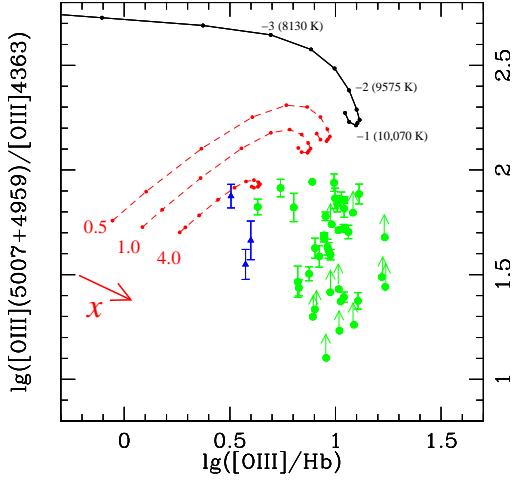


Figure 7. As Fig. 4, adding the hybrid AGN+stellar models (red, dashed lines) for different x values shown in red (0.5, 1.0 and 4.0).

Terlevich et al. 1991). Therefore, for the hybrid objects the $H\beta^*$ luminosities and equivalent widths expected from stellar photoionization are consistent with those measured for HII galaxies.

We must not forget that the continuum emitted by type 2 quasars is not necessarily stellar so that the measured level is an upper limit to the stellar continuum level and the EW values discussed above for $H\beta^*$ relative to the stellar continuum are lower limits. A more strict analysis would require a quantification of other possible contaminants, such as scattered light from the hidden AGN. Polarimetric information would be needed to characterize the nature of the continuum. Lacking this information, we can only say that the continuum level detected from the hybrid objects, where the stellar contribution is probably highest, is consistent with that expected from $H\beta^*$.

While this is a simplistic exercise and one cannot expect all type 2 quasars to have identical spectra of the stellar ionized gas, it suggests nevertheless that adding a varying contribution of stellar photoionized gas works in the right direction to solve most of the problems affecting the standard AGN sequence. The temperature problem remains and a more sophisticated scenario with a range of gas densities or the presence of a matter bounded component might be a viable solution.

Some studies suggest that the $[OIII]\lambda 5007$ emission line is an unbiased indicator of the intrinsic optical-UV luminosity of both type 1 quasars and radio galaxies. (Simpson 1998). According to the results above, it is possible that $[OIII]$ has a strong stellar contribution in a fraction of type 2 quasars. Let us estimate the fraction of $[OIII]$ flux originated by stars in the hybrid objects. We know that:

$$\frac{[OIII]^{tot}}{H\beta^{tot}} = \frac{[OIII]^{tot}}{[OIII]^*} \frac{[OIII]^*}{H\beta^*} \frac{H\beta^*}{H\beta^{tot}}$$

using $\frac{[OIII]^{tot}}{H\beta^{tot}}$ in the range 3.2-3.9 as measured for the hybrid objects, $\frac{[OIII]^*}{H\beta^*}=2.9$ (as for UM448) and $\frac{H\beta^*}{H\beta^{tot}}=0.8$ (since $x=4$) and rearranging, $\frac{[OIII]^*}{[OIII]^{tot}} \sim 59-72\%$. This suggests that there could be a fraction of type 2 quasars in which $[OIII]$ is not a reliable indicator of AGN power. Other type of studies should be performed to investigate this issue more carefully (e.g. Simpson 1998).

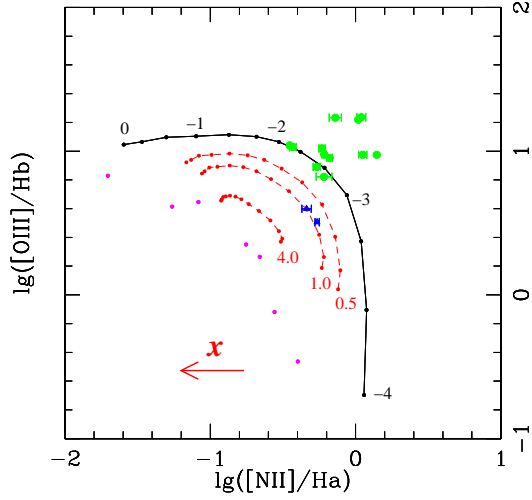


Figure 8. As Fig. 3 with the hybrid models.

4 DISCUSSION AND CONCLUSIONS

We have compared the optical emission lines ratios of type 2 quasars from Zakamska et al. (2003) with standard AGN photoionization model predictions, Seyfert 2s, HII galaxies, and narrow line FRII radio galaxies. Moderate to high ionization narrow line radio galaxies and Seyfert 2s are indistinguishable from type 2 quasars based on their optical line ratios. The standard AGN photoionization models, valid for other type 2 AGNs, can reproduce successfully the loci and trends of type 2 quasars in some of the main diagnostic diagrams. On the other hand, these models are not exempt of problems and the discrepancies with the data are the same encountered for other type 2 AGNs. The comparison between models and data suggests that a range of ionization and probably physical properties must exist within the type 2 quasar sample. An internal range of cloud properties (e.g. varying density) must also exist in individual objects. This is only natural, as one cannot expect identical gas and continuum properties (e.g. ionizing luminosity) in all quasars, or ensembles of identical clouds in individual objects.

Realistic models must take this into account. Possible solutions which have been extensively discussed in the literature are locally optimally emitting clouds, a mixture of matter and ionization bounded clouds, dusty, radiation-pressure dominated models or a mixture of clouds with different U values.

The relevant role played by AGN photoionization is not surprising, since Zakamska et al. (2003) selected objects with properties characteristic of active galaxies. However, based on the lack of correlation between $[OIII]$ and radio luminosities, other authors have suggested that an important fraction of type 2 quasars might not be dominated by AGN activity but by star formation (Vir Lal & Ho 2007; see also Kim et al. 2006).

We have found that stellar photoionization is obvious in a small fraction of objects (3 out of 50) which are characterized by low $[OIII]$ luminosities and large $[OII]/[OIII]$ ratios compared with most type 2 quasars in the sample.

Zakamska et al. (2003) sample is strongly biased towards objects with high line luminosities ($L[OIII] > 10^{42} \text{ erg s}^{-1}$). $L[OIII]$ can be as low as $\sim 10^{40} \text{ erg s}^{-1}$ in radio-quiet type 1 quasars and narrow line radio galaxies (e.g. Bennert et al. 2002, Tadhunter et al. 1998). There must be many type 2 quasars with $L[OIII]$ in the range $\sim 10^{40-42} \text{ erg s}^{-1}$. The hybrid objects discussed here, where

stellar photoionization is obvious, have among the lowest L[OIII] values within the type 2 quasar sample of Zakamska et al. (2003). This tentatively suggests that stellar photoionization could be relatively more important in type 2 quasars with lower [OIII] luminosities. If these objects have lower power AGNs (e.g. Simpson 1998), it would seem plausible to find a relatively higher contribution of the stellar photoionized gas to the observed emission line spectrum. The fraction of hybrid objects, therefore, could be much larger, if lower L[OIII] values were considered.

Since star formation has been found in different classes of type 2 AGNs at different z (e.g. Holt et al. 2007, Tadhunter et al. 2005, Alonso-Herrero et al. 2008) and in at least a fraction of type 2 quasars (Martínez-Sansigre et al. 2008, Lacy et al. 2007), stellar+AGN photoionization is a plausible scenario. Inspired by these arguments, we have explored an alternative scenario to pure AGN photoionization in which a varying contribution of stellar ionized gas is added to the line fluxes in type 2 quasars. Although the hybrid models presented here are rather simplistic and no reliable quantitative results can be extracted about the relative importance of stellar vs. AGN photoionization, they reproduce the type 2 quasar ratios (and type 2 AGN in general) quite successfully (better than the standard AGN sequence). This suggests that stellar photoionization might also be present in many type 2 quasars, in addition to AGN photoionization. Given that other type 2 AGNs have similar line ratios, this applies as well in those cases. On the other hand, and contrary to the more sophisticated AGN models discussed in the literature, the hybrid models cannot solve the “temperature problem” (see §3.1 B). Regarding all other line ratios, given the strong degeneracy with more sophisticated AGN photoionization models, it is not possible to favour one scenario or another in terms of the line ratios.

Other sources of information would be very valuable to test whether stellar photoionization is present in type 2 quasars and characterize its importance relative to the AGN photoionization (e.g. evidence for extended star formation, possible correlations between star formation indicators and the line ratios which require a stronger contribution of stellar ionized gas, lower continuum polarization level in objects with hints of stellar photoionization from the line ratios, etc). If the emission lines, in particular [OIII] λ 5007 have a strong contribution of stellar photoionized gas, the [OIII] line might not be a good indicator of AGN power.

ACKNOWLEDGMENTS

The authors thank to an anonymous referee for useful comments which helped to improve the paper. The work by MVM has been funded with support from the Spanish Ministerio de Educación y Ciencia through the grants AYA2004-02703 and AYA2007-64712, and co-financed with FEDER funds. Thanks to Joanna Holt for providing the data set on radio galaxies. LB was supported by the CONACyT grant J-50296

REFERENCES

Allen M., Dopita M., Tsvetanov Z., Sutherland R., 1999, *ApJ*, 511, 686
 Alonso-Herrero A. Prez-González P. G., Rieke G., Alexander D. M., Rigby J., Papovich C., Donley J., Rigopoulou D., 2008, *ApJ*, 277, 127

Anders E. & Grevesse N., 1989, *Geochim. Cosmochim. Acta*, 53, 197
 Antonucci R., 1993, *ARA&A*, 31, 473
 Baldwin J., Philips M. & Terlevich R., 1981, *PASP*, 93, 5
 Baldwin J., Ferland G., Korista K., Verner D., 1995, *ApJ*, 455, L119
 Bennert N., Falcke H., Shchekinov Y., Wilson A., Wills B., 2002, *ApJ*, 574, L105
 Bennert N., Jungwiert B., Komossa S., Haas M., Chini R., 2006, *A&A*, 2006, 456, 953
 Binette L., Dopita M. & Tuohy I.R.; 1985, *ApJ*, 297, 476
 Binette L., Wilson A., Storchi-Bergmann T., 1996, *A&A*, 312, 365
 Clark N. E., Axon D. J., Tadhunter C. N., Robinson A., O’Brien P., 1998, *MNRAS*, 494, 546
 Contini M., Radovich M., Rafanelli P., Richter G.M., 2002, *ApJ*, 572, 124
 Diaz A.I., Prieto M.A., Wamsteker W., 1988, *A&A*, 195, 53
 Dopita M., Sutherland R., 1996, *ApJS*, 102, 161
 Dopita M., Groves B., Sutherland R., Binette L., Cecil G., 2002, *ApJ*, 572, 753
 Ferguson D. H., Korista K., Baldwin J., Ferland G., 1997, *ApJ*, 487
 Ferruit P., Binette L., Sutherland R. S., Pecontal E., 1997, *A&A*, 322, 73
 Ferruit P., Wilson A., Whittle M., Simpson C., Mulchaey J., Ferland G., *ApJ*, 1999, 523, 147
 Groves B., Dopita M., Sutherland R., 2004, *ApJSS*, 153, 75
 Holt J., 2006, PhD thesis, Univ. of Sheffield
 Holt J., Tadhunter C.N., González Delgado R., Inskip K., Rodríguez J., Emmonts B., Morganti R., Wills K., 2007, *MNRAS*, 381, 611
 Humphrey A., Villar-Martin M., Vernet J., Fosbury R., di Serego Alighieri S., Binette L., 2008, *MNRAS*, 383, 11
 Kim M., Ho L.C., Im M., 2006, *ApJ*, 642, 702
 Koski A., 1978, *ApJ*, 223, 56
 Kraemer S., Crenshaw D., 2000, *ApJ*, 544, 763
 Lacy M., Sajina A., Petric A., Seymour N., Canalizo G., Ridgway S., Armus L., Storrie-Lombardi L., 2007, *ApJ*, 669L, 61
 Martínez-Sansigre A., Rawlings S., Lacy M., Fadda D., Marleau F., Simpson C., Willott C., Jarvis M., 2005, *Nature*, 436, 666
 Martínez-Sansigre A., Lacy M., Sajina A., Rawlings S., 2008, *ApJ*, 674, 676
 Osterbrock D.E., 1989, *Astrophysics of Gaseous Nebulae and Active Galactic Nuclei*. University Science Books, Mill Valley, CA
 Ptak A., Zakamska N., Strauss M., Krolik J., Heckman T., Schneider D., Birnckmann J., 2006, *ApJ*, 637, 147
 Reyes R., Zakamska N., Strauss M., Green J., Krolik J., Richards G., Anderson s., Schneider D., 2008, submitted to *AJ* (arXiv:0801.1115)
 Robinson A., Binette L., Fosbury R.A.E., Tadhunter C.N., 1987, *MNRAS*, 227, 97
 Simpson C., 1998, *MNRAS*, 297, L39
 Szokoly G. P., Bergeron J., Hasinger G. et al., 2004, *ApJS*, 2004, 155, 271
 Tadhunter C.N., Fosbury R.A.E., Quinn P.J., 1989, *MNRAS*, 240, 225
 Tadhunter C.N., Morganti R., Robinson A., Dickson R., Villar-Martin M., Fosbury R.A.E., 1998, *MNRAS*, 298, 1035
 Tadhunter C.N., 2002, *Revista Mexicana de Astronomía y Astrofísica (Serie de Conferencias)*, 13, 213-221

- Tadhunter C., Robinson T., Gonzalez Delgado R., Wills K., Morganti R., 2005, MNRAS, 356, 480
- Terlevich R., Melnick J., Masegosa J., Moles M., Copetti M., 1991, A&AS, 91, 285
- Viegas S., Prieto A., 1992, MNRAS, 258, 483
- Villar-Martín M., Tadhunter C., Morganti R., Axon D., Koekemoer A., 1999, MNRAS, 307, 24
- Villar-Martín M., Tadhunter C., Morganti R., Holt J., 2005, MNRAS, 359, 5
- Vir Lal D., Ho L.C., 2007, in press. To appear in "The Central Engine of Active Galactic Nuclei", ed. L. C. Ho and J.-M. Wang (San Francisco: ASP); arXiv:0706.0148
- York D., Adelman J., Anderson J. et al., 2000, AJ, 120, 1579
- Zakamska N., Strauss M., Krolik J. et al. 2003, AJ, 126, 2125
- Zakamska N., Strauss M., Heckman T., Ivezić Z., Krolik J., 2004, AJ, 128, 1002
- Zakamska N., Strauss M., Krolik J. et al. 2006, AJ, 132, 1496
- Zhang Z., Dultzin-Hacyan D. & Wang T., 2007, MNRAS, 377, 1215